AERODYNAMIC STUDY OF A NEW DESIGNED HYPERLOOP

[1]Saswata Bhattacharya

[1]Master of Engineering Student, Aerospace Department, Anna University, Madras Institute of Technology, Chennai, Tamil Nadu 600044, India, s.bhattacharya.engineer@gmail.com

Abstract: Enabling trade, commerce, communication & establishment of civilization is one of the most important roles of transportation. Out of the five most important mode of transportation namely, Roadways, Waterways, Railways, Airways & Pipeline-ways here the main focus is on Pipeline-ways of transportation. Exploring the world at most affordable rate as well as at the earliest is the main focus of the transportation industry. This project is done to increase the effectiveness of the 5th mode of transportation, i.e., Hyperloop by minimizing the Drag Force & improving the Lift for the Pod by providing suitable ADD ON Devices as Fixtures and modifying the shape. The initial idea was to determine the actual drag coefficient and lift generated in the base model of the pod, finding the boundary layer thickness. It is comprising of 3 parts: Pod, Capsule & Compressor fan. The Pod, Capsule & Compressor Fan are designed using SOLIDWORKS 2018 & a detailed computational/numerical study is performed on ANSYS Fluent 2020 with Grid and Domain independent study. Detailed flow structures with all aerodynamic data are contemplated along with all numerical iterations' validation. A Model of Hyperloop Pod fixed within a Capsule Shell with a Compressor fan secured ahead is developed & tested in the wind tunnel accompanied by boundary conditions in ANSYS Fluent platform. Coefficient of Drag & Lift of the Hyperloop Pod with two types of Add-on Devices namely, Vertical fixtures and Airfoil fixtures etc are analysed at two different speeds - low speed (300 m/s) & high speed (320 m/s). Using data from the simulation, graphs are generated that revealed a curve. Four different cases my altering components with varying speed are mainly under focus i.e.,1) Compressor (Dynamic Analysis) 2) Vertical Fixtures for pod and shell capsule 3) Airfoil Fixtures for pod with capsule 4) Assembled Case. After receiving sufficient results, data for both speeds are compared. A significant improvement in the aerodynamic efficiency for Hyperloop System is observed. Using Airfoil Fixtures on Pod is of great benefit. Improvement in energy consumption is possible with the improvement of Lift due to Airfoil Fixtures. Faster the Speed more is the pollution, keeping this under main consideration the Hyperloop runs on Green Energy.

Keywords: Hyperloop, Fastest Transportation, Economical Transportation, Elon Musk, vacuum travel, Compressor Analysis, Aerodynamic Drag, CFD,

1. Introduction:

Aerodynamics is the branch of Fluid Dynamics that studies the movement of air when it interacts with solid objects.

Conventional transportations are of four different types: air, rail, road, and water. These modes of transportation are usually slow and expensive. A conceptual mode of transportation known as Hyperloop is proposed. It uses a near-vacuum tube to travel at speeds of over 300 kilometres per hour.

A low-pressure tube that carries capsules at low and high speeds over its entire length is the Hyperloop. The capsules float in mid-air on a pressurised air cushion with aerodynamic lift. The pods would employ a linear electric motor to accelerate gradually to cruising speed before gliding over the rail using passive magnetic levitation or air bearings.

Passengers can board and depart the Hyperloop at stations located at both ends or at branches of the tube's length. The Hyperloop has the potential to significantly revolutionise transportation, relieve traffic congestion, and cut global carbon emissions.

Due to the growing population, a mass commuting is an alternate mode of transportation that is not only rapid but also economical & it is desperately needed to meet the growing demand at affordable cost.

Several major areas, such as LA – SF and Kansas City – St. Louis, are expected to be connected as a result of new technology, which is expected to be launched in the next years (MO).

Hyperloop Projects In India,
1. Pune-Mumbai hyperloop connecting the two cities in 30 minutes.
2. Bangalore International Airport Ltd., Kempegowda International Airport to and from connecting line from the city.
3. Punjab MoU with the Punjab Transport Department signed in December 2019.

2. Study Reason & Scope of Work:

The impact of a future oil supply deficit is the worst. Fuel prices are skyrocketing, and the environmental impact due to the fossil fuels burning is growing. The future of transportation is electric propulsion.

Advantages: Due to levitation from the surface, ground resistance has been abolished. Air resistance reduction not only aids in vehicle speed improvement but also decreases energy consumption and so enhances vehicle stability. Aerodynamic drag is the resisting force encountered by a moving body in a fluid & have some impact at greater speeds. The aerodynamic drag coefficient is a critical component in determining how much drag the vehicle experiences.

The air around the body generates different Drag.

Pressure or Form Drag	: Due to Pressure Difference of Air Flowing over the Body
Induced Drag	: Drag due to Lift.
Wave Drag	: Due to Formation of Shock Waves
Skin Friction Drag	: Due to actual contact of Air Particles with Body Surface
Parasite Drag	: Due to Roughness of the Body

The capsules are propelled by linear electromagnetic motors and would levitate in the vacuum due to electromagnetic repulsion, which would create a strong enough field to lift them off the tracks. Due to the vacuum atmosphere, the amount of energy required to lift the pods is said to be quite low. The solar panel mounted above the tube will provide the whole electrical energy consumption for the linear induction motor, magnetic force, and compressor fan. As a result, it is environmentally beneficial and sustainable transportation.

As the environmental consequences of energy usage deteriorate drastically, public transit will become increasingly important in the years ahead. The challenges of regulating friction and air resistance, both of which become significant when cars approach high speeds, have historically stymied high-speed rail development.

To diminish the levitation effect caused by magnetization and other aerodynamic instabilities at high speeds, reduction of drag is needed, which in turn also reduces wind noise, and thus create lift forces.

The drag coefficient (Cd) and frontal area (A), as well as the Lift coefficient (CL), may all be modified by the designer.

This research attempts to create a novel design of the pod with aerodynamic elements of hyperloop, based on the body structure of nature's fastest birds and fish. The pod's conditions with and without the shell are evaluated at two distinct speeds. CFD analysis is used to lower the cost of the procedure by skipping costly testing. Under those conditions, the principal output is the aerodynamic drag. The aerodynamic drag force will be reduced if the Pod, Capsule shell, and other components are designed with the frontal area optimization. The information is examined to do additional study.

3. LITERATURE REVIEW

In the research by Mohammed Imran (2016) as well as N. Kayela (2014) hyperloop technologies mainly on the passenger transport system are discussed. The differences between the passenger-only and

passenger-plus-vehicle variants of the hyperloop is explained in detail which depicts two variants. The hyperloop's railway track and hyperloop stations are discussed.

Mark Sakowski (2016) compared present maglev technology to theoretical evacuated tube technology, concluding that the hyperloop is viable and, if correctly designed, has the potential to be substantially more energy efficient for pods travelling down the tube.

From the study by Jeffrey C. Chin and colleagues Open-Source Conceptual Sizing Models for the Hyperloop Passenger Pod is known. On doing improved study, it's found & revealed the multiple multidisciplinary connections that change two important components of the initial notion. For the pod to reach Mach 0.8, the pod travel speed and the tube cross-sectional area are related, causing the tube size to be about double the diameter of the initial specification. Second, ambient thermal interactions dominate the steady-state tube temperature, which are unrelated to the heat created by the pod compression mechanism.

The design of a hyperloop capsule with a linear induction propulsion system that is utilised to accelerate and decelerate the capsule was addressed by Ahmed Hodaib and Samar F. Abdel Fattah (May 2016) in their research results. Linear motors, like rotary synchronous motors, run on 3-phase electricity and can handle very high speeds, according to the researchers. End effects, on the other hand, diminish the thrust force of the motor. For any needed force output, linear induction motors are thus less energy efficient than standard rotary motors. In the study, linear induction motors manufacturing process are also stated.

From Potla Jithendra's investigation, the Hyperloop system's construction features are known. The Hyperloop would be the first ground-breaking, one-of-a-kind transportation system in half a century, with the potential to drastically alter the time and cost equation for travel and transit between cities. The research has limits, including tube pressurisation, turning will be crucial, no response for equipment breakdown, accidents, and emergency evacuation from a safety standpoint.

The installation cost of High-speed rail and Hyperloop with others has been compared here. High-speed rail required more energy to power electromagnets for levitation and more lands are to be bought for the construction of high-speed rail whereas Hyperloop technology uses passive levitation which does not require energy to levitate and also, it's a self-powering system and needs less land for its construction. So, both the installation and maintenance costs will be very low. Different parts of the hyperloop system from the construction point of view are discussed. A slight tough of working principle is discussed. High Accessibility with a moderate capacity of travel as per comparison study.

4. Summary of Literature Review & Research Gap

Solar energy & wind kinetic energy are utilised through regenerative braking system, and in some regions, even eco-friendly thermal energy is utilised. It's now vital not just because it's environmentally friendly, but also because it saves more energy than it consumes, which is a significant benefit in addition to the cheap operating expenses.

Parts considered for the research from an aerodynamic standpoint Pods separately, Pods fixed to capsule shell, and compressor are to be revised for better performance.

Additional Hyperloop technical advancements and optimization might potentially lower the price even more. The effective speed at an appropriate pressure environment, where the least amount of drag is achievable, must be carefully determined. To save energy, the drag reduction methods obtained are far must be reduced with the improvisation of new techniques as well as some add on devices, fixtures, etc.

5. Design Research Detail Work

5.1 Design of Hyperloop and its Parts

Based on the Aerodynamic shape of nature's fastest animals the Pod has been designed. Keeping minimum gap, the shell is created, and 2 variations are given on the

attachments of the pod with the shell – Vertical Oval Fixtures & Airfoil Fixtures. A compressor Fan is created with mechanical coupling attached to the pod.

5.1.1 Design of Pod Model

Using Solid works 2018, all the detailing of the Base Model of the Hyperloop Pod is being drafted. Taking the help of the shape of nature's animals and the Virgin Hyperloop model, a scaled model has been achieved.

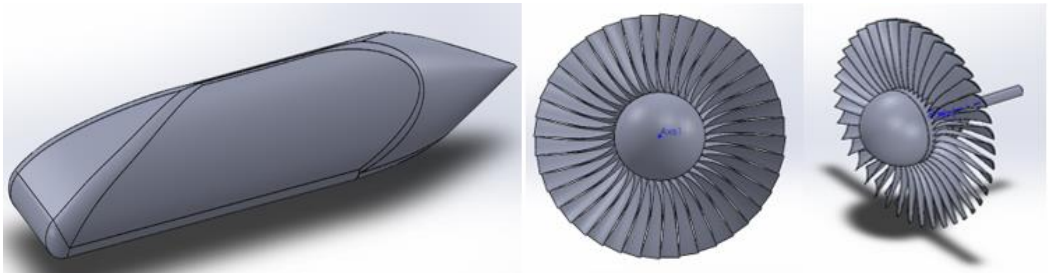

Figure 1 Pod Design & Compressor Fan

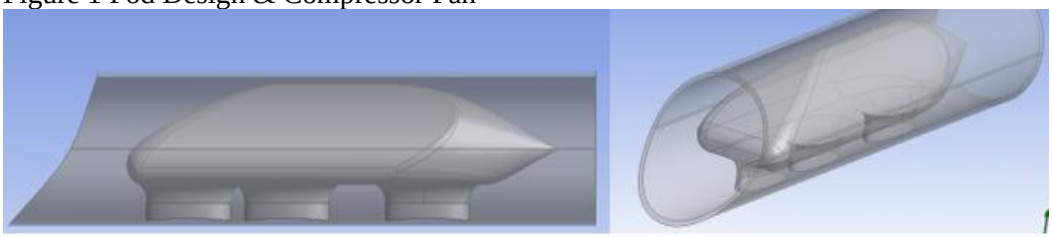

Figure 2 Pod with Vertical Fixtures within Shell

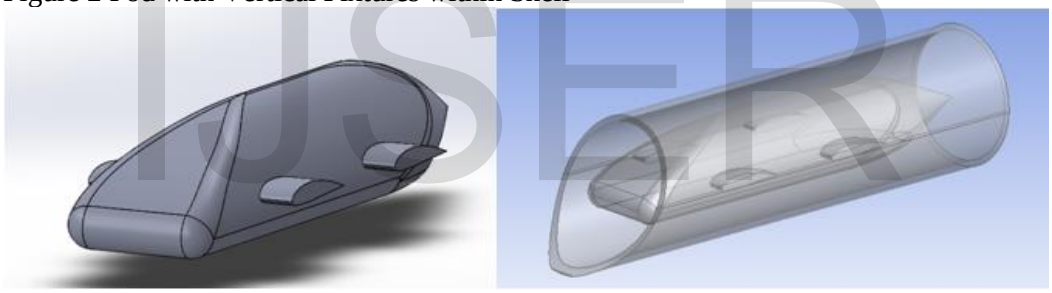

Figure 3 Pod with Airfoil Fixtures without & within Shell

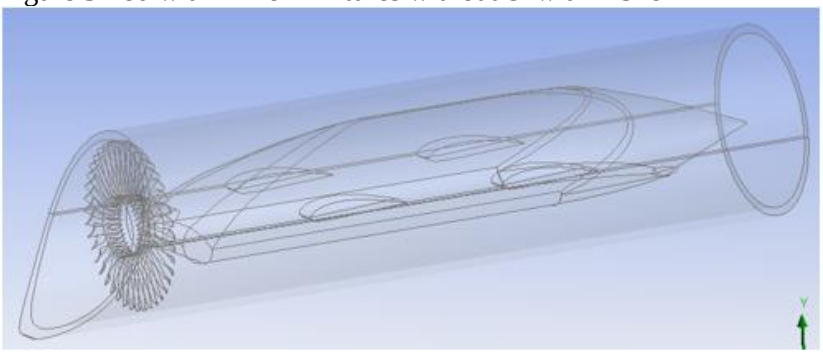

Figure 4 Pod with Airfoil Fixtures within Shell with Compressor Fan

5.2 Boundary Conditions

Temperature as 25° C or 298 K as per Indian Climate condition.

Accordingly,

Air Density for 25° C – 0.34555 Kg/cu.m

Air Viscosity for 25° C – 1.846E-05 Kg/ms or 1.837E-05 Kg/ms

Pressure – 30398 Pa or 0.3 ATM

Material - Aluminium, Air

Relative Humidity – 70 %

5.3 Manual Calculation of Drag Force of Actual Pod

FD = ½ * CD * P * A * V2

Where,

F_D – Drag Force
C_D – Coefficient of Drag
P – Density of Air @ particular Temperature
V – Velocity of Body or Fluid moving

Calculation Part

Density is 0.34555 Kg/m3 from chart.
C_D only for the Pod = 0.003 as per company data
Hydraulic Diameter = 0.157225556 m as per company data
Frontal Area = 0.123484663 sq m as per company data
Velocity Considered are 1) 320 m/s & 2) 300 m/s

Drag Force Calculation

F_D = 6.3 N for 320 m/s
F_D = 5.5 N for 300 m/s

5.4 Manual Calculation of Reynolds Numbers (Actual)

Air Kinematic Viscosity for 25^0 C – 1.84 x 10^{-5} sq m/s or 1.846E-05sq m/s
Air Dynamic Viscosity for 25^0 C – 1.923 x 10^{-5} sq m/s

Reynolds Number

It's the Inertial Force upon Viscous Force Ratio.

R_E = (PVL)/μ

Where,

Re = Reynolds Number
P = Density @ 25^0C
V = Velocity of Body or Fluid
L = Characteristics Linear Length
μ = Dynamic Viscosity of Fluid

Calculation Part

Density is 0.34555 Kg/m3 from chart.

Characteristics Length = 8700 m as per company data

Viscosity = 1.84 x 10-5 Kg/ms @ 250C

Velocity = 320m/s & 300 m/s

Reynolds Number Calculation

Re = 52113176.15@ 320 m/s

Re = 48856102.64@300 m/s

5.5 Comparison with Virgin Hyperloop Dimensions

DIMENSIONS (mm)	MODEL	PROTOTYPE
LENGTH	8700	306
BREADTH	2400	64
HEIGHT	2400	52

A dimensional comparison with model car and Actual Prototype:

Scale Model: 28.431 times (L)

Scale Model: 37.5 times (B)

Scale Model: 46.154 times (H)

APPROX. SCALING: 38 times

Figure 5 Model & Actual Comparison

5.6 Manual Calculation of Drag Force of Model Pod

Calculation Part

Density is 0.34555 Kg/m3 from chart.

C_D = 0.003 as per company data

Frontal Area = 0.002952277 sq m

Velocity Considered are 320 m/s & 300 m/s

Drag Force Calculation

F_D = 0.150428305 N

F_D = 0.132212377 N

5.7 Manual Calculation of Reynolds Numbers (Model)

Density is 0.34555 Kg/m3 from the chart.

Scaled Characteristics Length = 0.306 m

Viscosity = 1.84 x 10-5 Kg/ms @ 250C

Velocity = 320m/s & 300 m/s

Reynolds Number Calculation

Re = 1832481.421 @320 m/s

Re = 1717951.332 @300 m/s

5.8 Dimensions and Attachments of Fan or Compressor & Fixtures

5.8.1 Dimensions of the Compressor Fan

Table 1 Compressor Details - Design Dimensions

DIMENSION	Value
RADIUS (mm)	175
DIAMETER (mm)	350
RPS	500

5.8.2 Installation Positions

At the Front head of the Pod

5.9 Dimensions and Attachments of Fixtures of Pod with Capsule Shell

5.9.1 Dimensions of the Fixtures

5.9.1.1 Airfoil Fixtures Design

DIMENSION	Value
Breath (m)	0.009
Length (m)	0.05
Height (m)	0.001
Distance between (m)	0.01

5.9.1.2 Installation Positions of Airfoil Fixtures

Airfoil shaped 2 Fixtures are attached on either side of the pod i.e., sideways

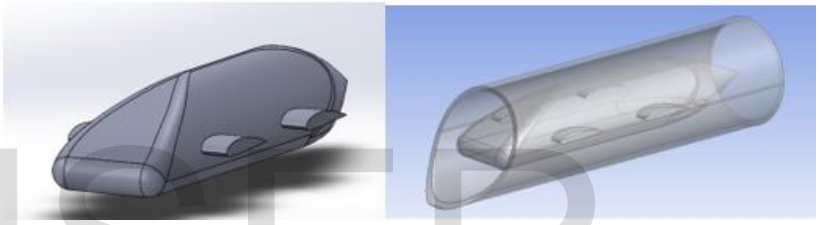

Figure 6 Airfoil Fixtures on either Side of Pod within the Capsule

5.9.1.3 Installation of Vertical Oval Shaped 3 Fixtures

Oval Shaped 3 Fixtures are attached with vertical upright beneath the pod with the capsule

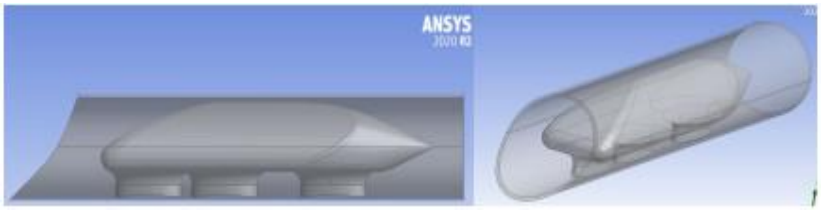

Figure 7 Vertical Fixtures beneath the Pod within Capsule

6. Analysis Research Detail Work

6.1 Analysis of Pod Base Model

1st the Base Model is chosen for analysis as well as the selection of the CFD model is done based on the following conditions.

With a turbulence intensity of 5%, the K-OMEGA turbulence model with SST function is utilised, along with the pressure-based Naiver Strokes equation (PBNS). The least square cell approach is used to discretize the semi-implicit pressure linked equation (SIMPLE). For all circumstances, the 2nd order upwind scheme governs pressure, momentum, turbulent kinetic energy, and turbulent dissipation rate. The K epsilon model is ideal for flow away from the wall, such as in the free surface flow zone, whereas the K -omega model is best for flow nearer to the wall, when an unfavourable pressure gradient develops. The K-w SST model has two equations. It solves two

transport equations in addition to the convergence equation (PDEs). It can illustrate turbulent energy convection or diffusion.

Two conveyed variables are as follows:
Turbulent kinetic energy (K) – defines the energy in turbulence.
Turbulent dissipation rate (w) – indicates the rate of dissipation per unit of turbulent kinetic energy.
Type of Study is Chosen: Grid & Domain-Independent Study
In general, grid and domain independence study has been performed to find that at some mesh there will be less difference or same values tries to repeat. For our case, three different cylindrical control volume sizes are chosen and performed the analysis from coarse to fine mesh (tetrahedral). Hyperloop is running through the tunnel, which is a hollow cylinder, due to which cylindrical Domain is chosen for analysis

Different Domains Taken for Domain-Independent Study

1st Domain
Positions in the Domain
Front & Rear to Pod surface : 500 mm
All sides from Pod walls : 250 mm

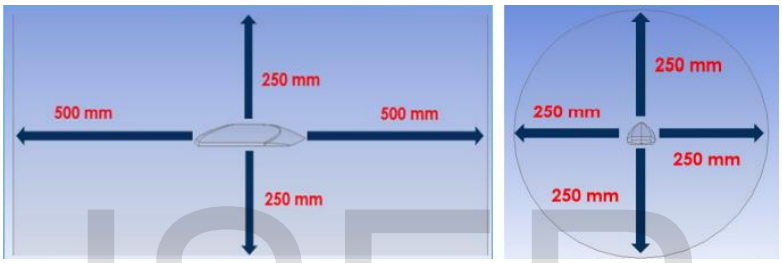

Figure 8 1st Domain Dimensions

2nd Domain
Positions in the Domain
Front & Rear to Pod surface : 500 mm
All sides from Pod walls : 200 mm

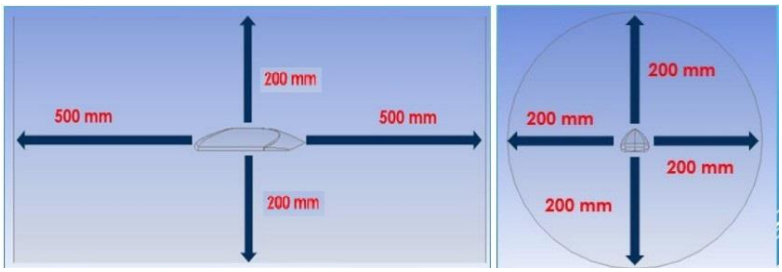

Figure 9 2nd Domain Dimensions

3rd Domain
Positions in the Domain
Front & Rear to Pod surface : 500 mm
All sides from Pod walls : 200 mm

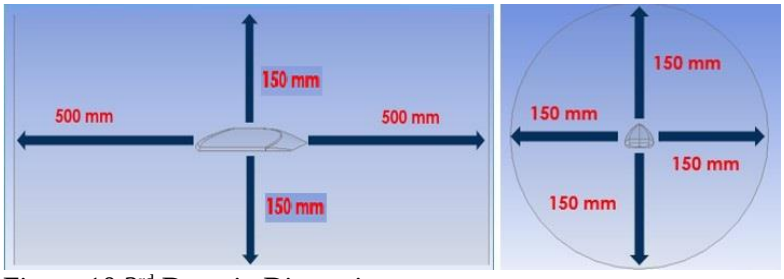

Figure 10 3rd Domain Dimensions

6.1.1. Different Grid Sizes Taken for Grid Independent Study

Table 2 Mesh Grid Sizes

SL. No.	Mesh Domain (mm)	Mesh Pod (mm)
1	65	1
2	60	0.9
3	55	0.8
4	50	0.7
1	65	1

A total of 4 grid sizes are chosen for the study for each domain.

Mesh Quality is high. Pod Faces & edges are being meshed, and the Domain faces and edges are being meshed. Gradually, from course mesh to fine mesh the study is performed.

After Grid Independent, study for each Domain the Results has been achieved.

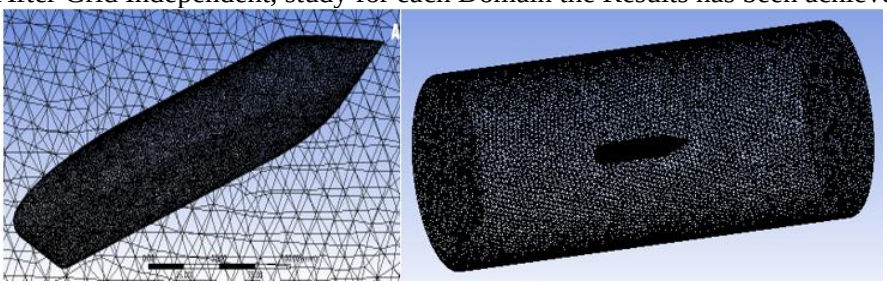

Figure 11 Pod Mesh & Mesh Domain as Solid Frame & Wireframe

The minimum percentage of variation among the cases 1 case is selected for each Domain for 320 m/s and 300 m/s.

6.1.2. Mesh Attributes

The meshing technique used for CFD domain construction was chosen to keep the meshing quality attributes of element quality, skewness, and orthogonality within the range as per Ansys' meshing material.

Table 3 Mesh Quality Range

SL No.	DOMAIN	Domain Mesh Grid Size (mm)	Pod Mesh Grid Size (mm)	MESH TYPE	ORTHOGONAL QUALITY	SKEWNESS
1	1ST DOMAIN	65	1	COURSE	0.69733	0.24695
2		60	0.9	LESS COURSE	0.71065	0.2454
3		55	0.8	LESS FINE	0.72183	0.24354
4		50	0.7	FINE	0.72856	0.24476
1	2nd DOMAIN	65	1	COURSE	0.69795	0.24628
2		60	0.9	LESS COURSE	0.71241	0.24383
3		55	0.8	LESS FINE	0.72123	0.24421
4		50	0.7	FINE	0.72912	0.2443
1	3rd DOMAIN	65	1	COURSE	0.69704	0.24716
2		60	0.9	LESS COURSE	0.71095	0.24526
3		55	0.8	LESS FINE	0.72117	0.24411
4		50	0.7	FINE	0.72854	0.24478

Mesh quality is checked so that the analysis of different types of geometry which depicts mesh discretization so that there is any convergence issue or not, helps areas for mesh improvements, etc.

The orthogonality measure ranges from 0 (bad) to 1 (good): (0.6 to 0.8) – very good acceptable range.

The lower the maximum skewness, the better the mesh. skewness less than 0.5 is average & 0.1 are very good: (0.3 to 0.1) – very good mesh.

6.2 Analysis of Basic Pod Model for 2 different velocities

For Velocity **320** m/s

Table 4 Results of varying Domain Sizes (320m/s)

Domain 1st							
Coefficient of Drag	Coefficient of Lift	Pressure Drag Force (N)	Viscous Force (N)	Drag Force (N)	Pressure Coefficient	Y+ (mm)	Y* (mm)
0.0534365	-0.0185597	1.570692	1.2204132	2.7911047	0.030071351	32	25
Domain 2nd							
Coefficient of Drag	Coefficient of Lift	Pressure Drag Force (N)	Viscous Force (N)	Drag Force (N)	Pressure Coefficient	Y+ (mm)	Y* (mm)
0.0557538	-0.0167298	1.697282	1.21486	2.9121424	0.032494971	29	23
3rd Domain							
Coefficient of Drag	Coefficient of Lift	Pressure Drag Force (N)	Viscous Force (N)	Drag Force (N)	Pressure Coefficient	Y+ (mm)	Y* (mm)
0.0590649	-0.0162235	1.8236343	1.26145	3.0850842	0.03491401	26	21

For Velocity **300 m/s**

Table 5 Results of varying Domain Sizes (300m/s)

Domain 1st							
Coefficient of Drag	Coefficient of Lift	Pressure Drag Force (N)	Viscous Force (N)	Drag Force (N)	Pressure Coefficient	Y+ (mm)	Y* (mm)
0.05449011	-0.012757	1.50668183	1.3394544	2.8461361	0.02884587	30	23
Domain 2nd							
Coefficient of Drag	Coefficient of Lift	Pressure Drag Force (N)	Viscous Force (N)	Drag Force (N)	Pressure Coefficient	Y+ (mm)	Y* (mm)
0.05933343	-0.0139524	1.5261463	1.3752403	2.9013866	0.03119519	27	22
3rd Domain							
Coefficient of Drag	Coefficient of Lift	Pressure Drag Force (N)	Viscous Force (N)	Drag Force (N)	Pressure Coefficient	Y+ (mm)	Y* (mm)
0.06625396	-0.0178961	1.60474518	1.4367864	3.0415315	0.03495631	25	20

Inference from domain & grid independence study

From this grid and domain independence study, we could observe that from coarse to the fine mesh, values for domain1, the percentage (-2.19023 %) for velocity 320 m/s and values for domain2, the percentage (-0.02552%) for velocity 300 m/s of different values are lesser than others, and the values try to repeat at that marked element size, hence those specified values for further studies have been taken.

Hence, for further analysis for 320 m/s & 300 m/s, with finer element size (55,0.8) mm has been selected, to capture flow separation cure.

Table 6 Analysis Comparison of Base Model & Prototype

Velocity 320 m/s				Velocity 300 m/s			
	Model	Prototype	% Change		Model	Prototype	% Change
Cd	0.05449011	0.003	-0.000514901	Cd	0.05933343	0.003	-0.000563334
Fd	2.8461361	6.29195312	0.03445817	Fd	2.9013866	5.530036924	0.026286503

Analytical Explanation through Illustrations

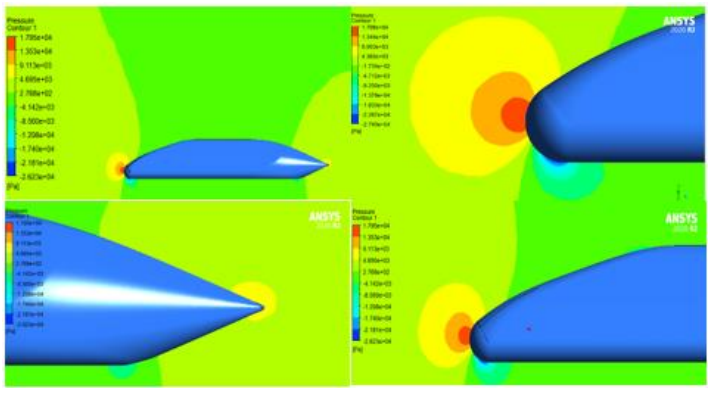

Figure 12 Pressure contours - Base Model Pod

Red Couture shows very high-pressure generation. As the couture is getting lighter, the pressure is less. At the rear end, there is less pressure. Thus, there is a generation pressure drag but less. The pod is sucked behind

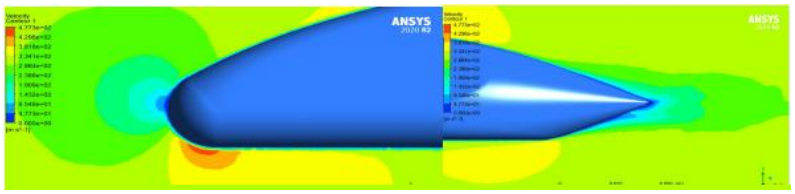

Figure 13 Velocity Contours at Pod Base Model

High Velocity depicting in the red region. Generation of wake at the rear end of the vehicle. Generation of moderately high velocity at the top forward slant as well as the rear top end slant.

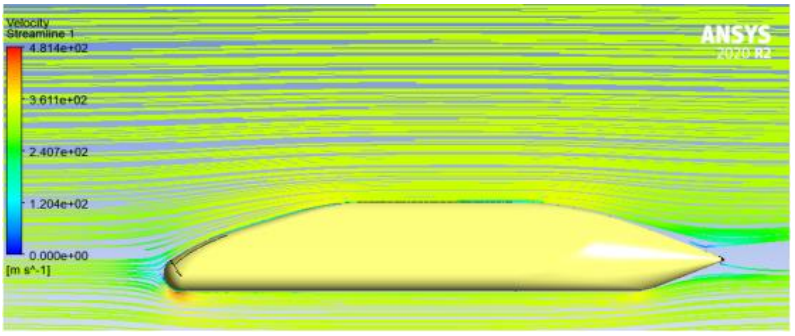

Figure 14 Streamline Motion: Side View (Pod Base Model)

From the Streamline Motion pictures of the Base Model, there is a generation of circulation behind the vehicle which is a very bare minimum. It is a minimum restriction for the pod to move forward.

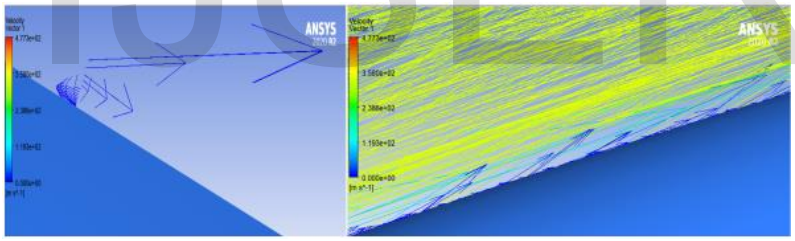

Figure 15 Vector Flow Lines: Zoomed Side View (Base Model)

From the Vector Flow pictures of Zoomed Pod Base Model, the vector lines are backward, so the flow is attached to the surface of the body. After a certain thickness, the flow is reversed. Boundary layer thickness is observed.

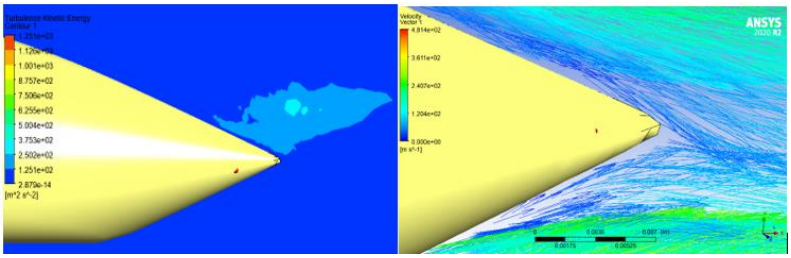

Figure 16 Turbulence Kinetic Energy & Turbulence Kinetic Energy: Rear End

GRAPHICAL REPRESENTATIONS

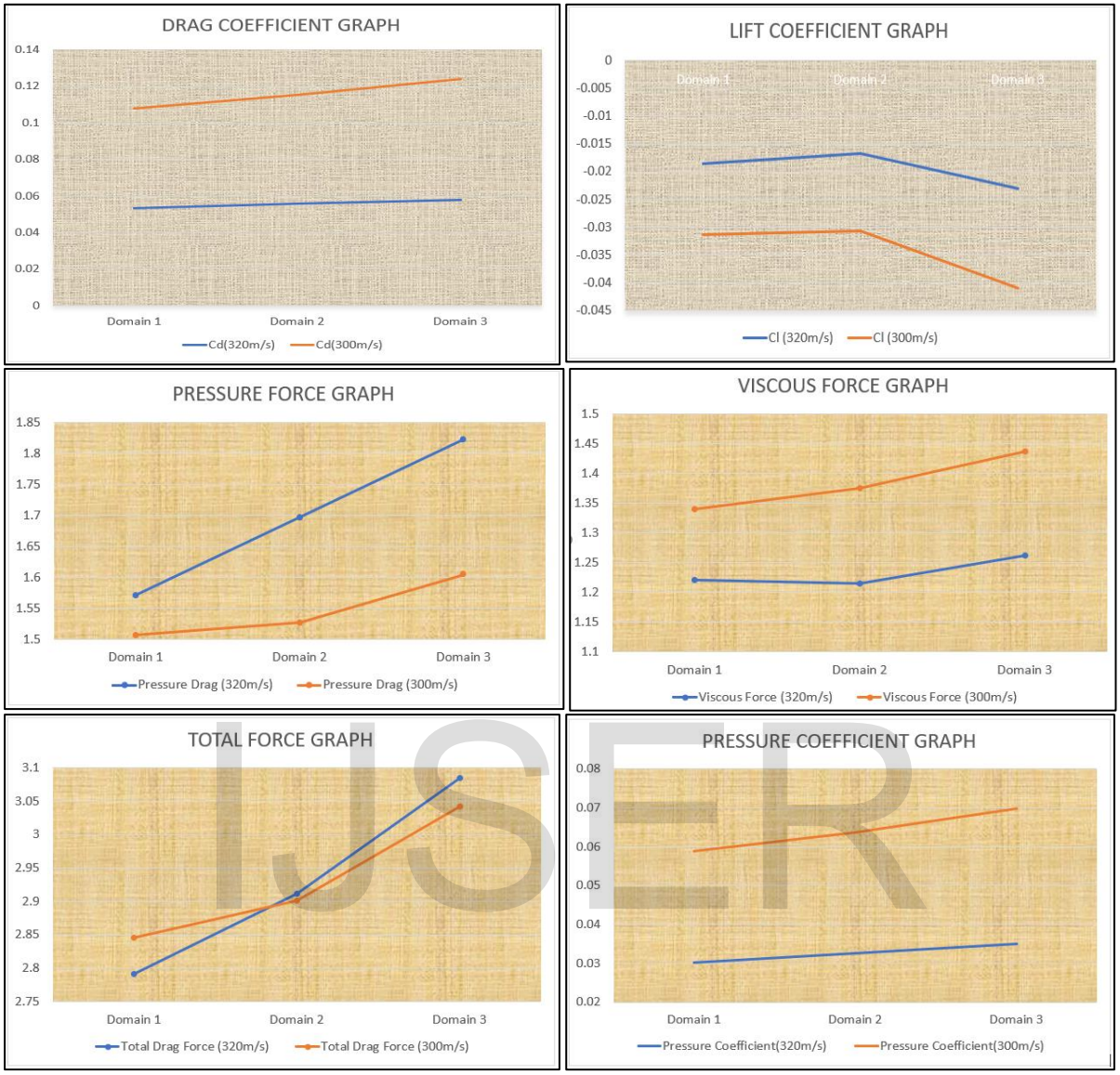

Velocity 320 m/s is more effective than 300 m/s at 0.3 ATM pressure.

6.3 Analysis of Compressor Fan – Fixed at the Front of the Hyperloop Pod

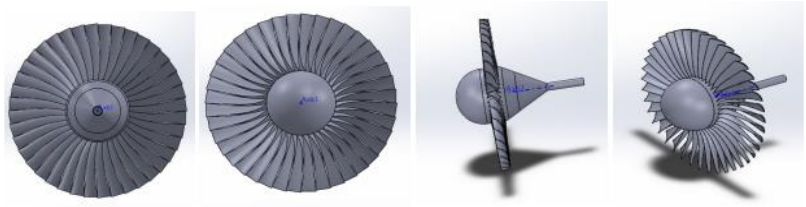

Figure 17 360-degree View Face of Designed Compressor Fan

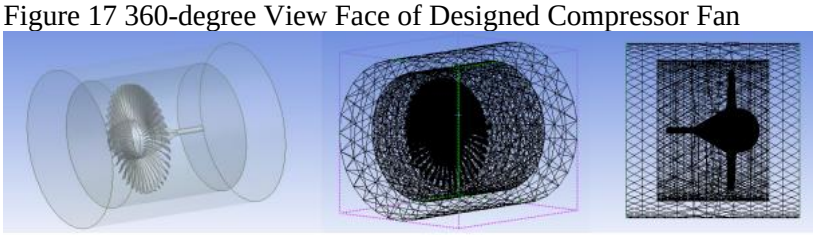

Figure 18 Two Domains & Compressor Fan Mesh

The Quality check is done for the following enclosures created for the dynamic CFD analysis of the Compressor Fan.

Dimensions & Quality check

Table 7 Dimensions of Enclosures for Analysis

ENCLOSURE	**Dimensions Name**	**Dimensions**
ENCLOSURE 1	RADIUS	30 mm
	Length	30 mm
ENCLOSURE 2	RADIUS	50 mm
	Length	100 mm

Table 8 Mesh Attributes for Compressor

SURROUNDING MESH SIZE	ROTATING REGION MESH SIZE	FAN MESH SIZE	NODES	ELEMENTS	ORTHOGONAL QUALITY	SKEWNESS
60 mm	25 mm	2 mm	2151035	2303715	0.75806	0.24048

Analysis of Compressor Fan for two velocities

For velocity 320 m/s & 300 m/s

Table 9 Analysis Result of Compressor Fan - velocity 320 m/s & 300 m/s

Analysis for Velocity **320 m/s**							
Coefficient of Drag	Coefficient of Lift	Pressure Drag Force (N)	Viscous Force (N)	Drag Force (N)	Pressure Coefficient	Mass Flow Rate (kg/s)	Mass-Weighted Average Velocity Magnitude (m/s)
0.0183482	-0.0307728	8.506701	0.0212574	8.527958	0.0160385	21.35425	330.43115
Analysis for Velocity **300 m/s**							
Coefficient of Drag	Coefficient of Lift	Pressure Drag Force (N)	Viscous Force (N)	Drag Force (N)	Pressure Coefficient	Mass Flow Rate (kg/s)	Mass-Weighted Average Velocity Magnitude (m/s)
0.0171052	-0.0335325	9.0208368	0.0247753	9.045613	0.0170584	22.776253	352.40956

Analytical Explanation through Illustrations

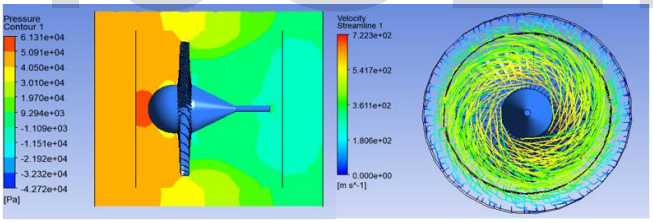

Figure 19 Pressure Contour & Rotational Velocity Streamline Profile - Compressor
From Red area to yellow to Green, change of High Pressure to Low Pressure. Some low pressure is observed at the rear end of the Compressor coupling with the Pod. The Compressor is generating low pressure at the rear end helping the Pod to move forward by pressure difference.

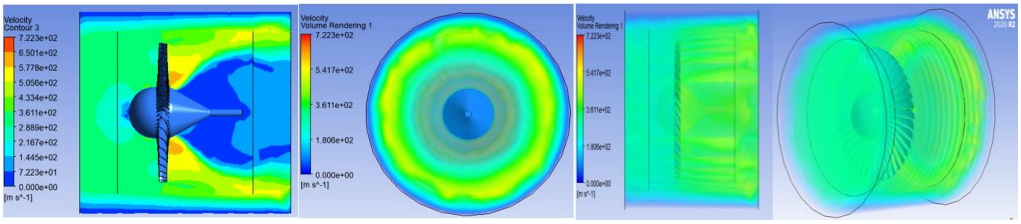

Figure 20 Velocity Couture & Velocity Volume Rendering Vision (3D)
The rear end is depicting an increase in velocity. High-speed fluid flow is observed by the red and gradually to the yellow region. Due to the presence of the rear body gradually decreasing the space via slant the velocity has decreased but not stopped – sky blue & deep blue is representing this.

GRAPHICAL REPRESENTATIONS

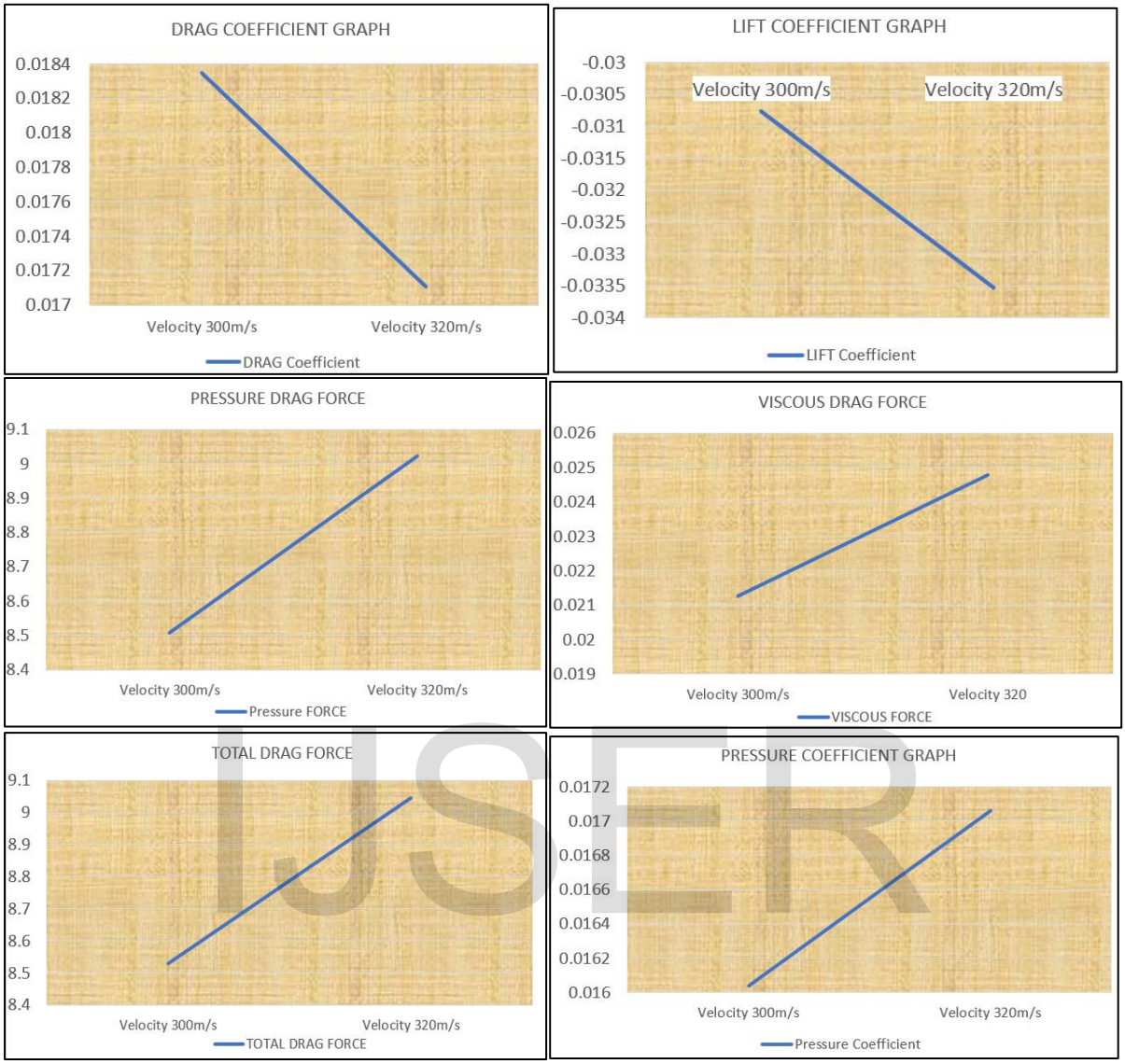

For the compressor fan the speed of linear flow is of 320 m/s and rpm of 500 rps is more effective for which the drag is less.

6.4 Analysis of Hyperloop Pod - Vertical Fixtures with Pod & Capsule

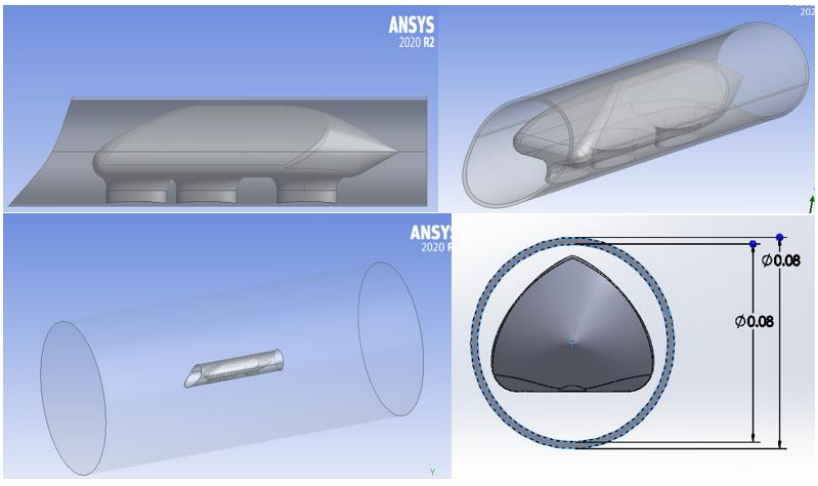

Figure 21 Vertical Oval Fixtures attaching Pod with Shell & Cylindrical Domain

With the introduction of the shell around the pod, the mesh grid size is altered. Keeping the quality of the mesh under an acceptable region the simulation is processed.

The Quality check is done for the following enclosure for the dynamic CFD analysis of the Pod fixed Capsule Shell for Domain 1.

Quality check

Table 10 Mesh Attributes for Vertical Fixtures Pod & Capsule

SL. No.	SURROUNDING MESH SIZE	POD REGION MESH SIZE	NODES	ELEMENTS	ORTHOGONAL QUALITY	SKEWNESS
1	70 mm	1.1 mm	974182	5154362	0.77025	0.22805
2	75 mm	1.2 mm	816031	4309909	0.77012	0.2282

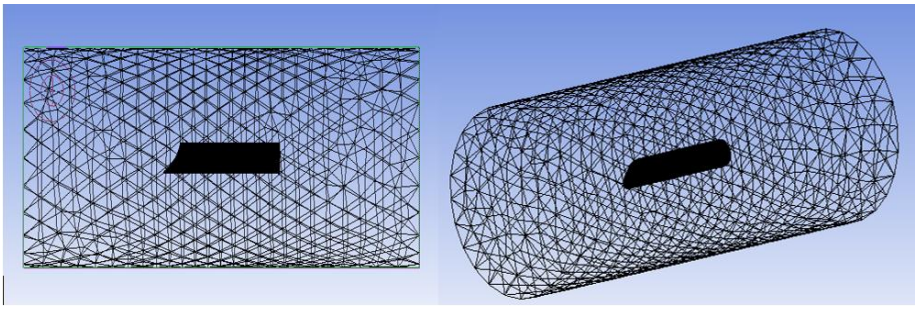

Figure 22 Mesh for Vertical Fixtures with Pod Model

Analysis of Pod & Shell being attached with Vertical Fixtures for two velocities

For velocity **320 m/s & 300 m/s**

Table 11 Analysis Result of Vertical Fixtures - velocity 320 m/s & 300 m/s

Analysis for Velocity **320 m/s**							
Coefficient of Drag	Coefficient of Lift	Pressure Drag Force (N)	Viscous Force (N)	Drag Force (N)	Pressure Coefficient	Y+ (mm)	Y* (mm)
0.57735168	-0.0528862	46.300633	18.3856345	64.686268	0.41352475	71.5	69
Analysis for Velocity **300 m/s**							
Coefficient of Drag	Coefficient of Lift	Pressure Drag Force (N)	Viscous Force (N)	Drag Force (N)	Pressure Coefficient	Y+ (mm)	Y* (mm)
0.50735495	-0.0373451	41.2860135	16.1616965	57.44771	0.36462138	67.2	68

Analytical Explanation through Illustrations

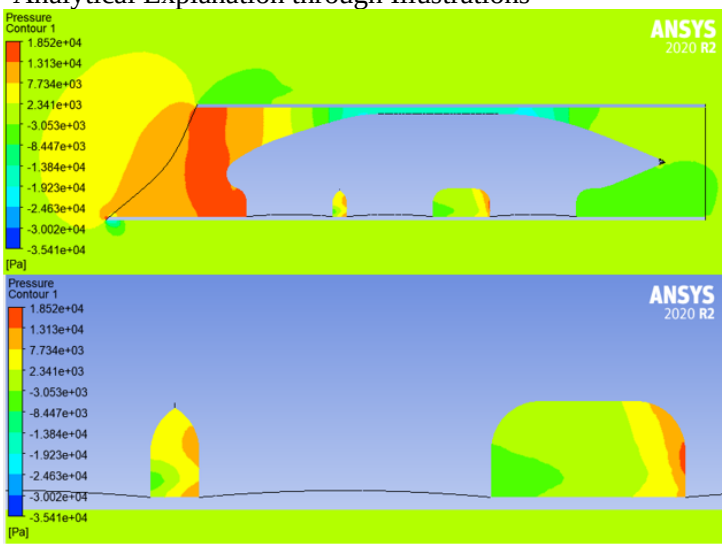

Figure 23 Local Pressure Contour & Zoomed at the Oval Vertical Fixtures

Low Pressure at the rear of the vehicle. Red zone depicting high pressure & Green zone as low pressure. At the Fixtures, the red contours are representing a high-pressure generation. At the rear fixtures, green is representing the low-pressure region. The rear end of the pod is representing a low-pressure region with a green contour. Top of the pod its negative pressure generation due to the flow-through a constricted area which will help in lift generation.

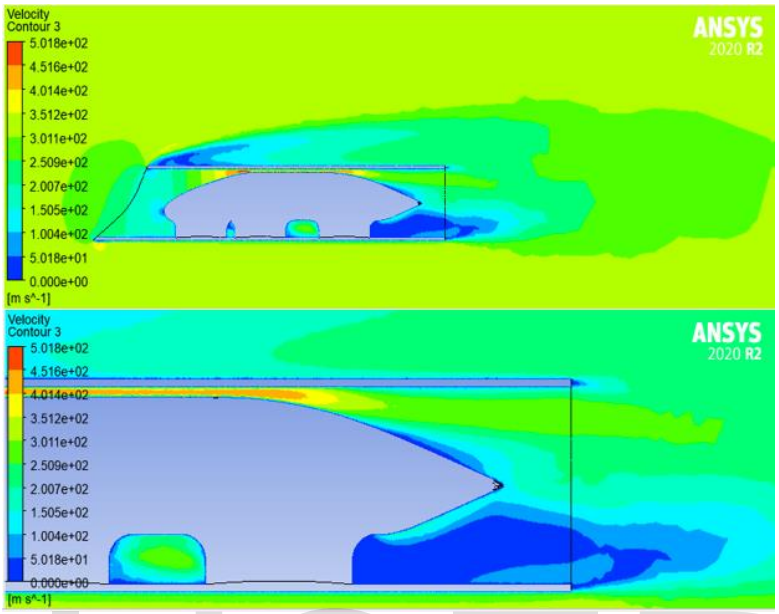

Figure 24 Velocity Contour & Zoomed at the Oval Vertical Fixtures (Rear)

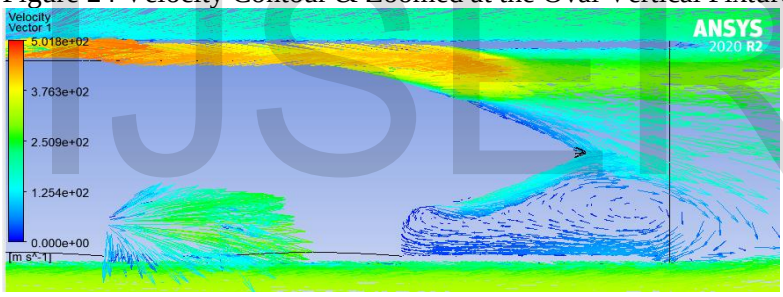

Figure 25 Velocity Vector Zoomed at the Oval Vertical Fixtures (Rear)

There is a generation of circulation at the rear end generated due to the vertical fixtures. Due to the slanted rear end, the flow is attached to the surface and the generation of a wake is low. High flow velocity is there at the top constricted area – represented by red and yellow vector lines.

6.5 Analysis of Hyperloop Pod - Airfoil Fixtures with Pod & Capsule

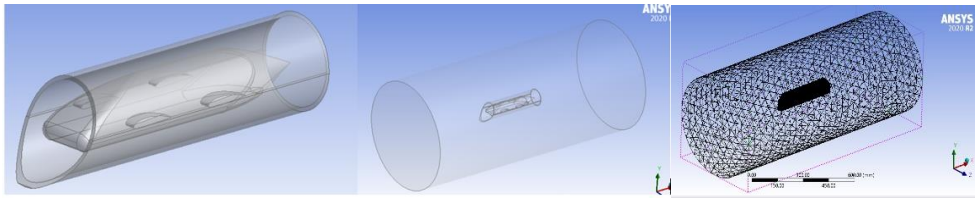

Figure 26 Pod with Airfoil Fixtures in a Cylindrical Enclosure & Meshing

With the introduction of the shell around the pod, the mesh grid size is altered. Keeping the quality of the mesh under an acceptable region the simulation is processed.

The Quality check is done for the following domain and enclosure for the dynamic CFD analysis of the Pod fixed Capsule Shell for Domain 1

Table 12 Mesh Attributes for Airfoil Fixtures attached to Pod & Capsule

SL. No.	SURROUNDING MESH SIZE	POD REGION MESH SIZE	NODES	ELEMENTS	ORTHOGONAL QUALITY	SKEWNESS
1	70 mm	1.1 mm	983019	5217467	0.76976	0.22855
2	75 mm	1.2 mm	825413	4376316	0.76925	0.22909

Mesh Quality is under acceptable range for both Orthogonality and skewness factor.

Analysis of Pod & Shell being attached with Airfoil Fixtures for two velocities

For velocity 320 m/s & 300 m/s

Table 13 Analysis Result of Airfoil Fixtures - velocity 320 m/s & 300 m/s

Analysis for Velocity **320 m/s**							
Coefficient of Drag	Coefficient of Lift	Pressure Drag Force (N)	Viscous Force (N)	Drag Force (N)	Pressure Coefficient	Y+ (mm)	Y* (mm)
0.50136876	-0.0281944	39.501019	20.67632	60.177339	0.32912142	74	75
Analysis for Velocity **300 m/s**							
Coefficient of Drag	Coefficient of Lift	Pressure Drag Force (N)	Viscous Force (N)	Drag Force (N)	Pressure Coefficient	Y+ (mm)	Y* (mm)
0.469664	-0.023934	34.592624	18.4067765	52.961744	0.53002116	70	71

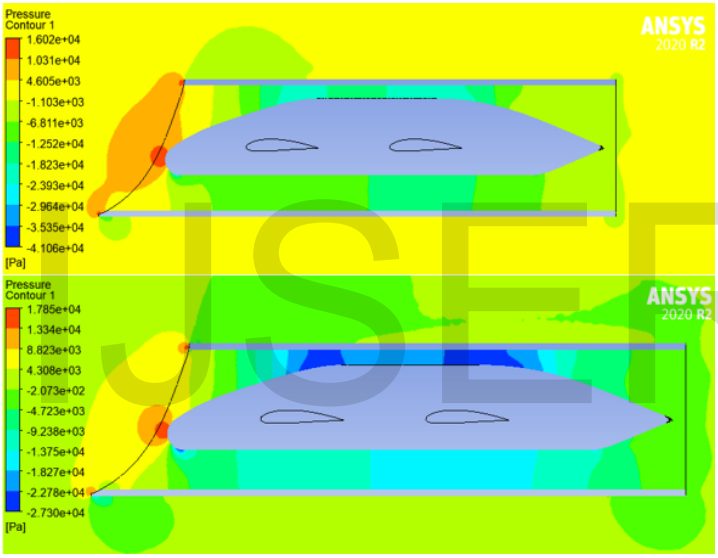

Figure 27 Global & Local Pressure Contour for Airfoil Fixtures mid region

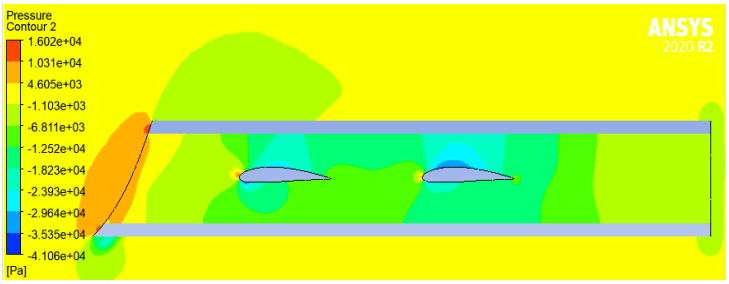

Figure 28 Pressure Contour for Airfoil Fixtures over the Airfoil region

From the pressure contour – High-pressure generation at the head of the pod with low-pressure generation at the top of the pod due to flow through the constricted area and thus creating an upliftment. Low pressure at the rear end and thus creating backward suction. The Airfoil is generating low lift but better performance than vertical fixtures.

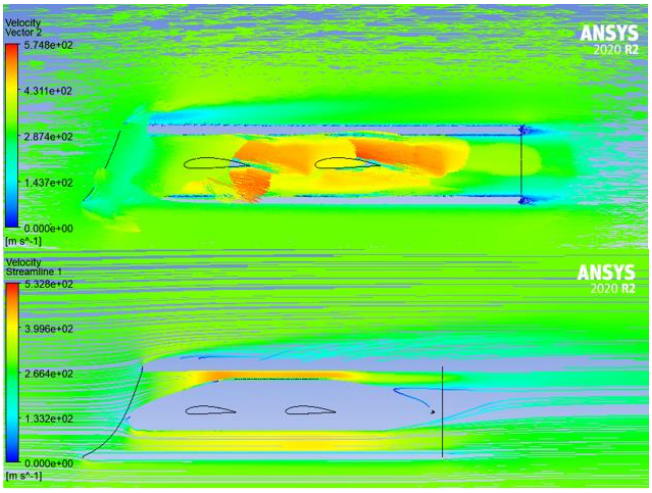

Figure 29 Velocity Contour & Streamline Flow for Airfoil Fixtures mid region

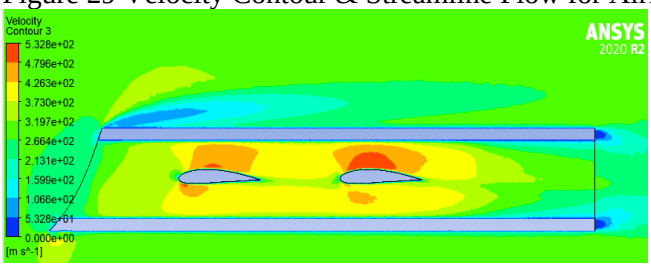

Figure 30 Velocity Contour Airfoil Fixtures Airfoil region

High velocity is there over the Airfoil with a low velocity at the lower surface region of the Airfoil thus according to the energy equation the pressure at the lower surface is more than the pressure at the upper surface so there's a generation of upward force which generates lift to the pod.

SPECIFICATION OF AIRFOIL:

For the generation of the lift and reduction of drag force here NACA 3124 Airfoil is used.

In detail : NACA 3412 Airfoil M=3.0% P=40.0% T=12.0%

Here, M = Max Camber (%), P = Max camber position (%), T = Thickness (%)

GRAPHICAL REPRESENTATIONS with COMPARISON

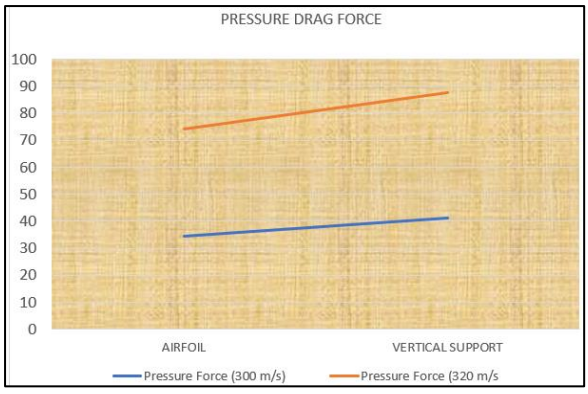

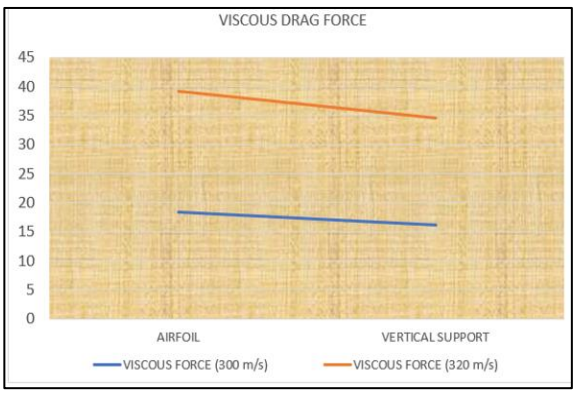

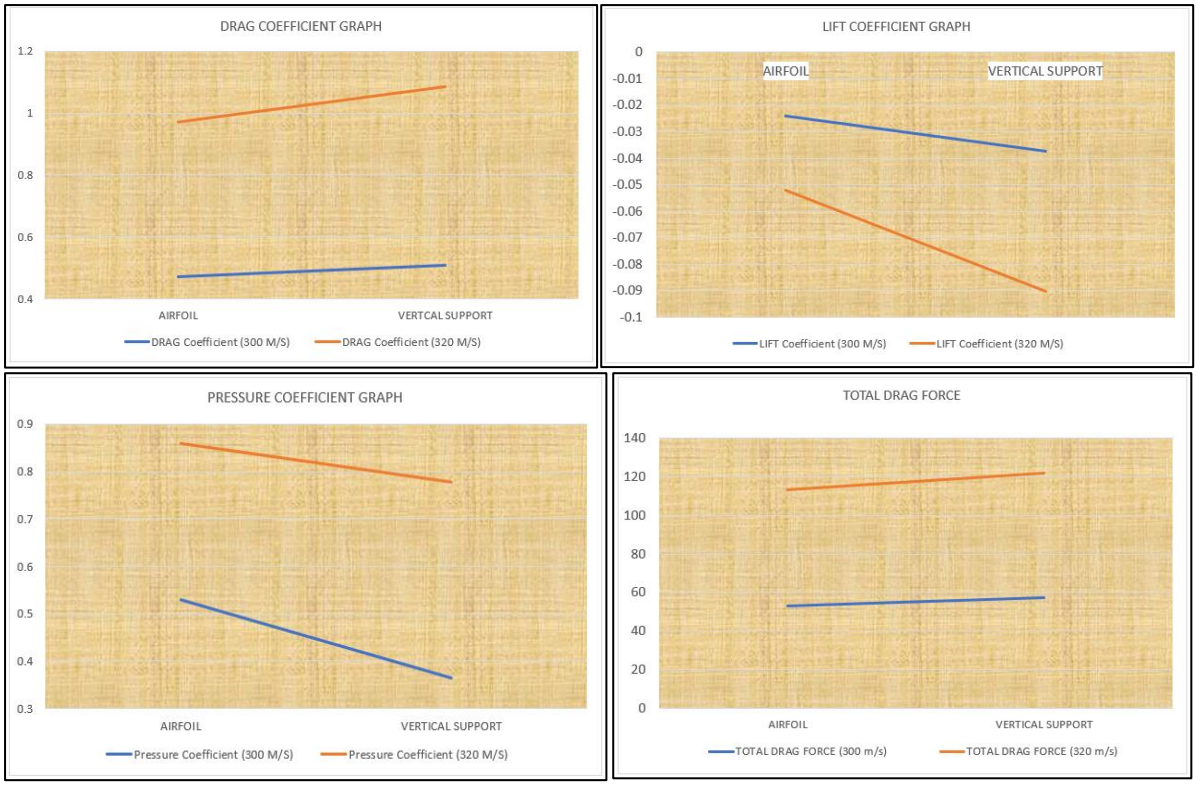

The drag coefficient with airfoil is less than Vertical fixtures.
The Lift coefficient with airfoil is more than vertical support.
The total force generated with vertical fixtures is more than the Airfoil fixtures.
So effective fixtures to be used for the pod to fix with the capsule issuing the NACA 3412 Airfoil shaped fixtures.
The Compressor fan fixed with the pod and capsule is done and simulated for effective result.

6.6 Analysis of Assembled Parts with Hyperloop Pod

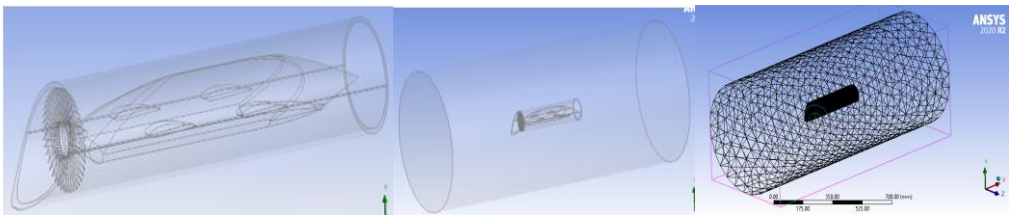

Figure 31 Design of Pod Fixed Capsule with Airfoil Fixtures, Compressor & Meching

With the introduction of the Capsule shell around the pod & the Compressor made the mesh grid size is altered. Keeping the quality of the mesh under an acceptable region the simulation is processed.

The Quality check is done for the following domain and enclosure for the dynamic CFD analysis of the Pod fixed Capsule Shell for Domain 1.

Table 14 Mesh Attributes for Final Assembled Pod

SL. No.	SURROUNDING MESH SIZE	POD REGION MESH SIZE	NODES	ELEMENTS	ORTHOGONAL QUALITY	SKEWNESS
1	75 mm	1.2 mm	937804	4967120	0.76958	0.22877
2	80 mm	1.3 mm	792803	4194479	0.76935	0.22899

Mesh Quality is under the acceptable range for both Orthogonality and skewness factors.

Analysis of Assembled Pod-Shell being attached with Airfoil Fixtures & Compressor

For velocity 320 m/s & 300 m/s

Table 15 Analysis Result of Final Assembled Pod - velocity 320 m/s & 300 m/s

Analysis for Velocity **320 m/s**							
Coefficient of Drag	Coefficient of Lift	Pressure Drag Force (N)	Viscous Force (N)	Drag Force (N)	Pressure Coefficient	Y+ (mm)	Y* (mm)
0.73476034	-0.0604717	84.6866925	16.3591975	101.04589	0.6158036	72	73
Analysis for Velocity **300 m/s**							
Coefficient of Drag	Coefficient of Lift	Pressure Drag Force (N)	Viscous Force (N)	Drag Force (N)	Pressure Coefficient	Y+ (mm)	Y* (mm)
0.73619833	-0.060075	74.3893525	14.5943205	88.983672	0.61545354	68	69

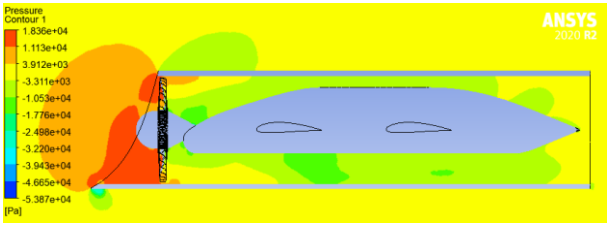

Figure 32 Global Pressure Contour for Final Assembled Hyperloop Pod

High Pressure is generated at the Front – Red to Orange region is showing thus. Low Pressure is generated at the top & bottom of the pod. Whereas pressure at the top is relatively lower than the pressure at the bottom. The rear is having low pressure thus a backward suction will be created.

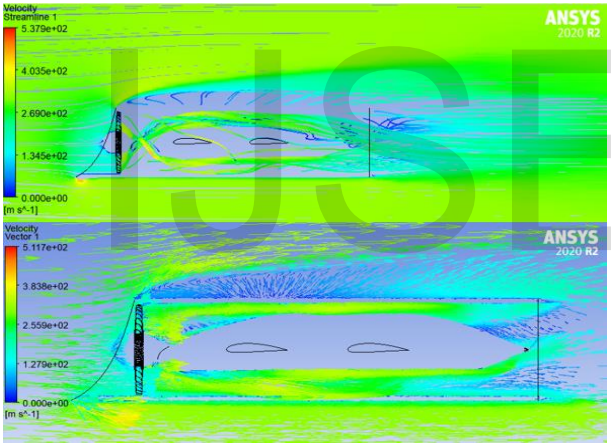

Figure 33 Velocity Streamline flow & Vector Lines for Final Assembled Hyperloop Pod

From the vector lines, it was observed there is a circulation being created at the rear end. The top rear slanted surface is an area of the circulation thus pressure is low, and suction is created which is to be eliminated.

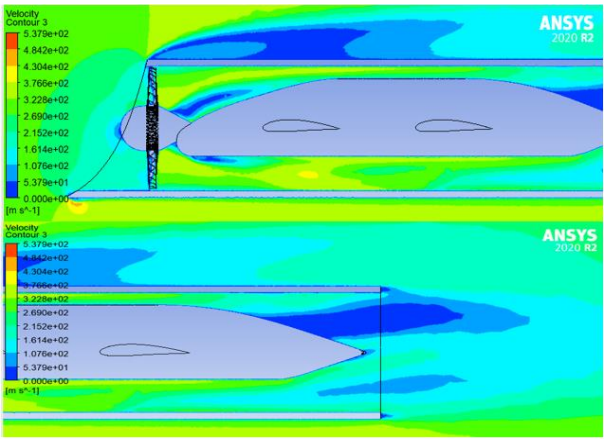

Figure 34 Velocity Contour for Final Assembled Hyperloop Pod (zoomed front & rear)

Wake is created at the rear top slanted area. Due to which the performance is down. With the application of some add-on devices, this can be improved.

The blue region is showing the fluid with very little velocity. The change of velocity happened suddenly after the constricted area.

The problem is found well from the velocity contour, vector, and Pressure Contour Regions.

Comparison Graph for Final Assembled Pod with Speed Variation

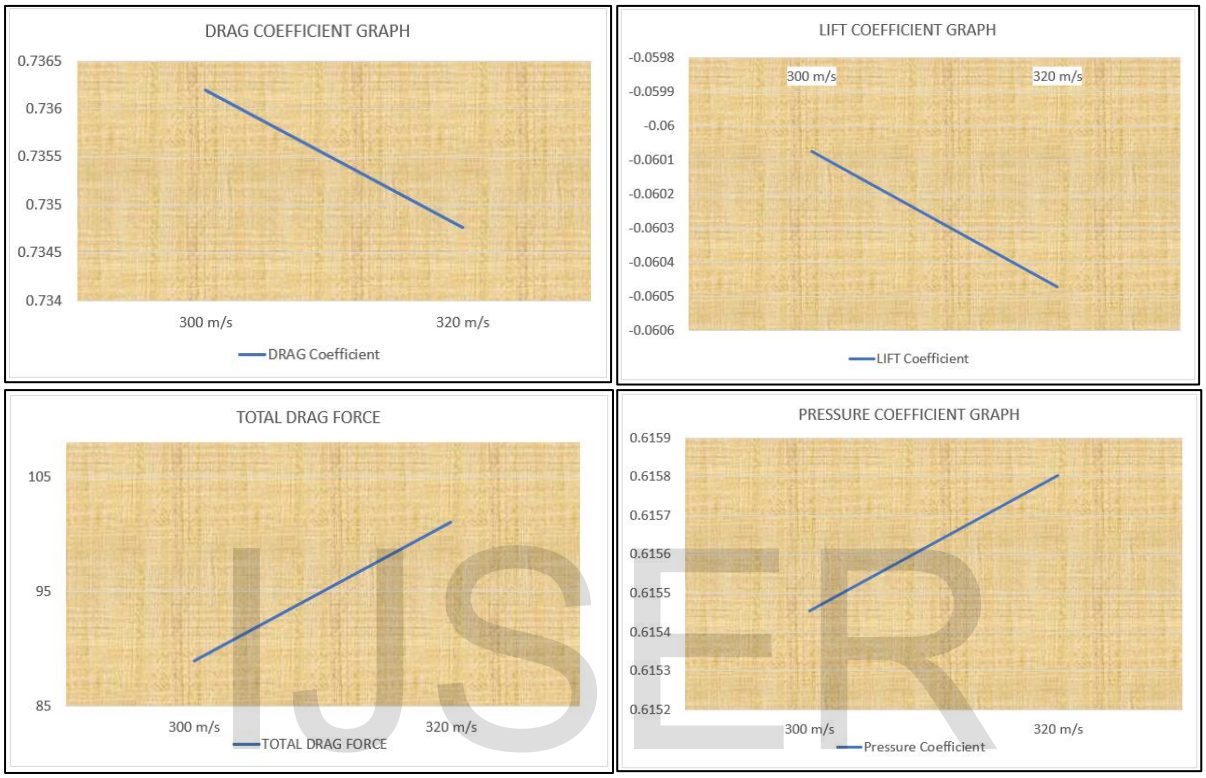

7. Results and discussion

7.1. INFERENCE

As per the Final Assembled Hyperloop Pod, Analysis the Coefficient of drag observed is 0.73619833 (300 m/s) & 0.73476034 (320 m/s).

The drag coefficient at 320 m/s is less than 300 m/s.
The Lift coefficient at 320 m/s is less than 300 m/s.
The total force generated at 320 m/s is more than 300 m/s.
The most effective fixture is the Airfoil Fixtures, which has reduced the Drag Coefficient a lot by 13% approximately than vertical Fixtures for 300 m/s & 8% for 320 m/s.

- Drag Reduction is to be done for the full POD – CAPSULE SYSTEM WITH FAN
- Lift is to be generated more for easy elevation.

7.2. VALIDATION

Computational models can provide results that aren't based on reality. As a result, the outcomes must always be scrutinised. There are two sections to the validation. The first section will be a grid refinement study, followed by a comparison of the acquired results to predicted data or existing research articles.

Grid refinement study

The coarse mesh model and the fine mesh model are utilised for grid refining. At least three meshes are required for a good grid refinement research. However, I employed two analyses for the Hyperloop Set due to the divergent result of the 3rd analysis. The change in lift and drag with decreasing mesh size is investigated for the grid refinement research. The purpose

of the assignment is to get these numbers, the lift and drag coefficient were chosen to be examined.

Table 16 Grid Refinement Study for Pod

Considering - Pod Only - 300 m/s						
Case	Number of elements	Factor of refinement	Lift	Change	Drag	Change
Coarse main model	32,66,000	1.959239743	-0.03486	56.59%	0.05719	5.70%
Fine main model	63,98,877		-0.01513		0.053933	

7.3. EXPLANATIONS

For Pod & Hyperloop Assembly

It demonstrates that the coarse mesh was still too coarse. The mesh refinement of factor of 1.959 & 1.2 respectively results in a change in lift of 56.59 & 9.24 percent respectively and a change in drag of 5.7 & 0.76 percent respectively. When the difference in lift and drag coefficients is less than 5% and the mesh is adjusted by a factor of 2, the grid is deemed fine enough. Because the coarse mesh was insufficiently fine, the primary hyperloop set model was reviewed and examined on a finer and less fine mesh, as provided. On a finer scale, the core model is assessed and studied. However, because the values of the coarse mesh grid are near to permissible levels, it is presumed that the grid is fine enough.

Comparison with other research papers

The produced lift should be in the order of magnitude of the hyperloop set's weight - Capsule. The Capsule's weight is 2.5 tonnes (actual-Virgin) which is 66 Kg here (scaled by 38 times), hence based on Airfoil fittings, one Airfoil should create roughly 16.5 N uplift force. The generated drag should be as low as possible in order to determine the magnitude of the compressor fan's thrust as well as the supply for the linear induction motor. The hyperloop set's drag force (Scaled Model) is 88.983672 N.

To validate my model and analysis, I compared the Cd and CL values with those of other research articles that used comparable scaling factors:

There are several papers where only the pod is used for the analysis whereas here both pod as an individual as well as pod being fix within the capsule with compressor fan set up for analysis. So according to available papers, the comparison is varied.

Table 17 Comparing with Different Research Papers

Parameters	Capsule Model Set Designed		Pod Model Designed		MIT HYPERLOOP FINAL REPORT		HYPERLOOP ALPHA		NUMERICAL ANALYSIS FOR AERODYNAMIC BEHAVIOUR OF HYPEROOP POD		HYPERLOOP CAPSULE CFD SIMULATION IN A CLOSED ENVIRONMENT	
					DATA	CHANGE	DATA	CHANGE	DATA	CHANGE	DATA	CHANGE
C_d -320m/s	0.7362	0.73548	0.0535	0.0564	0.0553	-1.92%	0.0431	-23.56%	0.0625	10.85%	0.064	13.51%
C_d -300m/s	0.7348		0.0594									
C_l -320m/s	-0.0605	-0.0603	-0.019	-0.017	-	-	-	-	-0.01	-38.48%	-0.02	23.03%
C_l - 300m/s	-0.0601		-0.014									

From the percentage differences of C_D value, the model is under the acceptable range.

C_L is not observed in many papers whereas in some it has been observed and compared.

8. Conclusion

CFD analysis carried out for Final Assembled Hyperloop Pod at 320 m/s & 300 m/s. For each velocity, I have analyzed 4 parts of the hyperloop system individually, namely Pod alone, Compressor Fan, Fixtures – Airfoil & Vertical fixtures with Pod and Capsule Shell.

A) Basic Hyperloop Pod model is aerodynamically analyzed and observed that the Drag coefficient is less at 320 m/s than 300 m/s. The lift coefficient for the 320 m/s is more than

that of the 300 m/s. Despite more pressure force drag at 320 m/s than 300 m/s, 320 m/s is more suitable from a productivity point of view.

B) The boundary layer thickness is observed from the mesh refinement study. For carrying out mesh refinement the first cell height/thickness must be calculated which was done using the below equation ie :

$$y^+ = \frac{yu_r}{m}$$

Where,
y - Absolute Distance
u_r - Friction Velocity
μ - Kinetic Viscosity

For calculating u_r, the below equation is used

1/7 power law & Schlichting equation is used to find Skin friction coefficient – Flat Plate & Non-Flat Plate

Based on Reynolds number the Equation Varies

1) Cf = 0.0576 Re-1/5 for 5*105 <Rex<107

2) Cf = [2log10(Rex)-0.65]-2.3 for Rex<109

Here,

Cf = 0.0576 Re-1/5 is used

Where,
Cf = skin friction coefficient
Re-Reynolds number of the fluid flow

$$\tau_w = \frac{1}{2}\left(c_f \rho u^2\right) \qquad u_r = \sqrt{\frac{\tau_w}{\rho}}$$

&

Where,
u = velocity of the fluid
p = density of the medium
After achieving T_w, u_r is calculated.

Table 18 First Thickness Layer (Y+ value)

Density [kg/m3]	Dynamic viscosity [kg/ms]	Boundary layer length [m]	Desired Y+ value	Reynolds number	Inflation layer	Estimated wall distance [m]
Velocity 320 m/s						
0.34555	1.82e-5	0.305922	20	1839904	20	2.80963E-05
Velocity 300 m/s						
0.34555	1.82e-5	0.305922	30	1717952	20	4.47101E-05

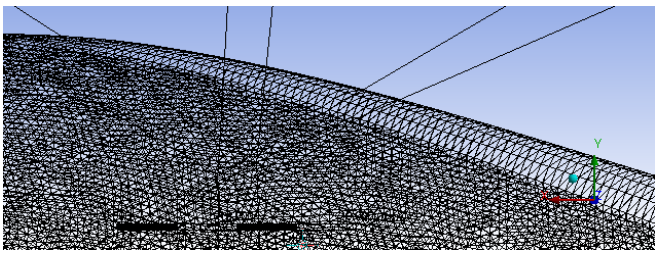

Figure 35 Mesh Inflation for boundary layer study

C) A compressor is fixed at the front of the Pod which is individually analyzed. Dynamic CFD analysis is carried out to achieve the result. With an outlet speed of 320 m/s is more effective than 300 m/s is observed.

D) Pod is attached to a capsule shell via two types of attachments namely Vertical Oval shaped attachments and Airfoil Attachments. With aerodynamic study, the Airfoil attachment fixture is more effective than Vertical attachments.

Table 19 Comparison of Vertical & Airfoil Fixtures

Comparison	Vertical Fixtures	Airfoil Fixtures	Difference (%) wrt Vertical Fixtures
Velocity 320 m/s			
Drag Coefficient	0.57735168	0.50136876	13.16059564
Lift Coefficient	-0.05288612	-0.02819436	46.68854512

Velocity 300 m/s			
Drag Coefficient	0.50735495	0.469664	7.428911455
Lift Coefficient	-0.03734504	-0.02393399	35.91119463

E) With Airfoil fixtures and the compressor, the Hyperloop Model is assembled, and the aerodynamic study is carried out at which the result is considered.

9. Future Work

The Airfoil Fixtures can be providing good Upward Lift with different angles.

More different types of Airfoil & more effective devices can be introduced to enhance the efficiency.

Modification in Airfoil Fixtures is needed. The angle of attack can be introduced for the effective Airfoil fixtures position. Inclusion of few more devices like Canards, Side Skirts, Vortex Generators to get the most effective results for the improvement of the Final Assembled model of Hyperloop Pod. Percentage Improvements in Drag Reduction is to be increased more than achieved. Percentage Lift reduction effectively should be more with minimum drag increase. Analysis with all effective Economical device attachments attached to the model. Improvement to Financial Expenses ratio should be feasible and affordable. Hyperloop is the breaking way of technology that will not only transform the mode of transportation only but will improve the quality of life and economy in the long run. Furthermore, transparent, and detailed research are needed for the establishment of the Hyperloop.

References

1. Ahmed Hodaib, Samar, et al, Conceptional Design of a Hyperloop Capsule with Linear Induction Propulsion System - International journal of mechanical, aerospace, industrial, mechatronics and manufacturing engineering Vol:10 No:5, (May 2016), pp 922 – 929, doi.org/10.5281/zenodo.1125541
2. Aditya Bose and Vimal K. Viswanathan, Mitigating the Piston Effect in High-Speed Hyperloop Transportation: A Study on the Use of Aerofoils, Energies, 2021, 14, 464. https://doi.org/10.3390/en14020464 pp 18
3. Chin, Jeffrey C.; Gray, Justin S, et el, (January 2015), Open-Source Conceptual Sizing Models for the Hyperloop Passenger Pod (PDF). 56th AIAA/ASCE/AHS/ASC Structures, Structural Dynamics, and Materials Conference. January 5–9, 2015. Kissimmee, Florida. doi:10.2514/6.2015-1587.
4. Mohammed Imran, international journal of engineering research, 2016
5. Musk, Elon (August 12, 2013). "Hyperloop Alpha"(PDF). SpaceX. Retrieved August 13, 2013
6. N. Kayela, editor of the scientific and technical department, “Hyperloop: A Fifth Mode of Transportation”, 2014
7. Potla Jithendra, (2015), Hyperloop Transportation System: A New Mode of Transportation - International Journal of Science and Research (IJSR) ISSN (Online): 2319-7064, pp 769 – 771
8. Paper by Mark Sakowski, “The Next Contender in High-Speed Transport Elon Musks Hyperloop”, 2016Wev
9. Pralhad Bhikaji Narkar1, et el, Review of Hyperloop Technology: A New Mode of Transportation, IJSRD - International Journal for Scientific Research & Development| Vol. 6, Issue 09, 2018 | ISSN (online): 2321-0613, pp- 73 75
10. Rajshri Tukaram Shinde, et el, Hyperloop Transportation System, International Research Journal of Engineering and Technology (IRJET), Apr -2017, pp- 763Md.- 766Md
11. Chauhan Aishwarya Dharmeshkumar, Patel Purvik Samir, Hyperloop: V Mode of Transportation. International Journal of Engineering Research & Technology (IJERT), VOLUME 10, ISSUE 02 (FEBRUARY 2021), Feb-2021, pp-543-546
12. Temoatzin González, et el, CFD Simulation of a Hyperloop Capsule Inside a Low-Pressure Environment Using an Aerodynamic Compressor as Propulsion and Drag Reduction Method, Applied Sciences 11(9):3934, DOI: 10.3390/app11093934
13. SuchithraRajendran & AidanHarper, A simulation-based approach to provide insights on Hyperloop network operations - Transportation Research Interdisciplinary Perspectives, Vol: 4, March 2020, 100092, Page 100307, doi.org/10.1016/j.trip.2020.100092
14. Ram Bansal & R. B. Sharma, Drag Reduction of Passenger Car Using Add-On Devices, Journal of Aerodynamics, Volume 2014, Article ID 678518, doi.org/10.1155/2014/678518
15. http://www.cikitusi.com/

16. VigneshS, Vikas Shridhar, et al, Windscreen angle and Hood inclination optimization for drag reduction in cars, Procedia Manufacturing, Volume 30, 2019, Pages 685-692, doi.org/10.1016/j.promfg.2019.02.062
17. FedericoLluesma-Rodríguez, TemoatzinGonzález, et el, CFD simulation of a hyperloop capsule inside a closed environment, Results in Engineering, Volume 9, March 2021, 100196, doi.org/10.1016/j.rineng.2020.100196
18. R. Fulton, A. I. Bishop, et el, Focusing ground-state xenon in a pulsed optical field, PHYSICAL REVIEW A, Vol. 71, Iss. 4 — April 2005, doi.org/10.1103/PhysRevA.71.043404
19. XuHui He, Zou Chao, Aerodynamic drag reduction of an Ahmed body based on deflectors, Journal of Wind Engineering and Industrial Aerodynamics 148:34-44, DOI: 10.1016/j.jweia.2015.11.004
20. Chen-Kang Huang, Performance Analysis and Optimized Design of Backward-Curved Airfoil Centrifugal Blowers, May 2009HVAC&R RESEARCH 15(3):461-488, DOI:10.1080/10789669.2009.10390846
21. Matt Stickland, Numerical flow simulation in a centrifugal pump with impeller - Volute interaction, Proceedings of ASME FEDSM'00 ASME 2000 Fluids Engineering Division Summer Meeting June 11-15, 2000, Boston, Massachusetts, June 2000
22. Katarzyna Gdowska, Rafał Rumin, Key Points of the Management System for the Safety of Passengers Travelling with Low-Pressure Trains, August 2020 New Trends in Production Engineering 3 (1):462-471, August 2020, DOI:10.2478/ntpe-2020-0039
23. Maurice Bizzozero, et el, Aerodynamic study of a Hyperloop pod equipped with the compressor to overcome the Kantrowitz limit, https://doi.org/10.1016/j.jweia.2021.104784
24. FIGURE 6: https://www.theverge.com/2020/11/8/21553014/virgin-hyperloop-first-human-test-speed-pod-tube